15 January 1996

OPTICS COMMUNICATIONS

ELSEVIER

Optics Communications 123 (1996) 225-233

Full length article

Nondiffracting beams: travelling, standing, rotating and spiral waves

S. Chávez-Cerda [1], G.S. McDonald, G.H.C. New

Laser Optics & Spectroscopy Group, The Blackett Laboratory, Imperial College of Science, Technology and Medicine, Prince Consort Road, London SW7 2BZ, UK

Received 23 May 1995

Abstract

A reformulation of nondiffracting beams, based on more general (travelling wave) solutions of the nonparaxial wave equation, is presented. Zero order nondiffracting beams are found to be radial standing waves arising from counterpropagating zero order Hankel waves of the first and second kind, while higher order nondiffracting beams are formed from counter-rotating spiral waves which are described by Hankel functions of the corresponding order. The resulting physical picture is more general than the well-known integral representation of Bessel functions and we expect it to have implications for studies of the applications of nondiffracting beams. Generic descriptions of the transverse profiles of the electric field, applicable to experimental configurations for realising nondiffracting beams, follow directly from this formulation. Finally, the existence of classes of periodically nondiffracting beams, possessing finite angular momentum and having the characteristics of rotating and spiral waves, is predicted.

1. Introduction

It was shown by Durnin et al. [1] that the Helmholtz equation for the free space propagation of light beams possesses exact eigenmode solutions that, in principle, describe beams which propagate indefinitely without any distortion due to diffraction. The problem is that these "nondiffracting" solutions, the simplest of which is proportional to the zero order Bessel function, are of infinite transverse extent and energy, and therefore cannot be realised in practice. However, Durnin et al. were able to demonstrate in experiments with beams of *finite* size that the characteristics of nondiffraction could be sustained over long distances [1].

Since this seminal work, there have been many experimental and computational investigations of the subject [2–4], all of which have adopted the original mathematical treatment of Durnin et al. in which the integral representation of the zero order Bessel function in the form of an azimuthal Fourier transform was used. On the other hand, interpretations of experiments on nondiffraction have relied either on ray diagrams (geometrical optics) or on Fresnel diffraction theory. The former technique is of course only valid in the limit where the optical wavelength, λ, is negligible compared to the characteristic length scales of the transverse patterns. Fresnel diffraction theory is considerably more general, but even then accounts only for *leading order* effects associated with finite λ. These limitations are unfortunate given that one of the most interesting attributes of nondiffracting beams is that they can sustain transverse structure that is of the order of λ in extent; this feature has potential applications in the detection and monitoring of very small objects for instance.

[1] Permanent address: Grupo de Fotónica, Instituto Nacional de Astrofisica, Optica y Electronica, Apartado Postal 51/216, Puebla, Mexico 72000.

SSDI 0030-4018(95)00538-2

In this paper we argue that the integral representation of nondiffracting beams is incomplete. This is mainly because of the fact that it can only represent a *stationary* transverse pattern of infinite transverse extent. Furthermore, this conventional representation has not, in previous studies, led to any new predictions or insight into the nature of nondiffraction. We show that a more general formulism leads to a more complete representation of aspects of the experimental realisation of nondiffracting beams and that it also lends itself to a generalisation of the concept of nondiffraction. More recently, Bessel beams have also been studied in the field of *nonlinear* optics [4,5] and many of the results that we report (those which concern only the nature of the light itself) also have application to these studies.

2. Solution of the wave equation

The context of this paper is the linear nonparaxial wave equation for scalar beams [6]

$$\nabla^2 E + k^2 E = 0, \tag{1}$$

where ∇^2 is the Laplacian in the spatial coordinates x, y and z, $k = \omega/c$ is the wavenumber, ω is the angular frequency and c is the speed of light. In the above, the harmonic time dependence, $\exp(-i\omega t)$, of the electric field has been removed. Seeking transverse eigenfunctions, one can also remove the rapid longitudinal variations of the field by setting $E = H(x, y)\exp(-ik_z z)$. Adopting now cylindrical coordinates (ρ, ϕ), such that $E = H(\rho)\exp(-ik_z z + im\phi)$, and substituting this ansatz into Eq. (1) yields

$$\rho^2 \frac{d^2 H}{d\rho^2} + \rho \frac{dH}{d\rho} + [(k^2 - k_z^2)\rho^2 - m^2]H = 0. \tag{2}$$

By defining a radial frequency, k_ρ, which is given by $k_\rho^2 = k^2 - k_z^2$, Eq. (2) can be immediately recognised as Bessel's equation.

It is at this stage in the derivation that most authors consider Bessel functions of the first kind, J_m, as the only physical solutions. However, Bessel's equation is a second order differential equation and thus has other solutions that are Bessel functions of the second kind, also known as Neumann functions, N_m. The reason why Neumann functions are not usually considered to be valid solutions is that, in isolation, they present singularities. However, in combination with Bessel functions, the Neumann functions can have both physical meaning and consequence. A particular linear combination of these solutions yields the mth-order Hankel functions, H_m, which are more general solutions to Bessel's equation than the Bessel functions themselves [7] and which, in our notation, take the form

$$H_m^{(1)}(k_\rho\rho) = J_m(k_\rho\rho) + iN_m(k_\rho\rho),$$
$$H_m^{(2)}(k_\rho\rho) = J_m(k_\rho\rho) - iN_m(k_\rho\rho). \tag{3}$$

The reciprocal of the free parameter, k_ρ, in the Hankel functions determines the length scale of the transverse structure of the solutions. For small values of k_ρ, transverse variation of the field is slow and geometrical optics is a useful approximation for describing some aspects of the propagating light. On the other hand, as $k_\rho \to k$, the transverse length scale approaches λ while, since $k_z \to 0$ at the same time, the phase variation of the beam along the z-axis disappears. It is in this limit that the central spot diameter of the nondiffracting beam becomes smaller than λ.

3. Travelling and standing waves

The Hankel functions of Eq. (3) describe *exact* travelling wave solutions of the *nonparaxial* wave equation. In the case of the zero order ($m = 0$) solutions, the first Hankel function $H_0^{(1)}$ describes radially-symmetric outgoing waves (travelling away from the axis) while $H_0^{(2)}$ represents incoming waves (travelling towards the axis). The type of radial symmetry which these waves possess is such that they are uniform in the azimuthal direction, ϕ. To demonstrate this, we consider the transverse beam profile at longitudinal locations such that $\exp(-ik_z z) = 1$. Thus, one can write $E = H(\rho) = H_0^{(1)} + H_0^{(2)}$ and, in terms of the total real field, $F(E) = (1/2)[E\exp(-i\omega t) + E^* \exp(i\omega t)]$, the individual zero order Hankel waves, $F(H_0^{(1)})$ and $F(H_0^{(2)})$, are

$$F_0^{(1)} = J_0(k_\rho\rho)\cos(\omega t) + N_0(k_\rho\rho)\sin(\omega t),$$
$$F_0^{(2)} = J_0(k_\rho\rho)\cos(\omega t) - N_0(k_\rho\rho)\sin(\omega t). \tag{4}$$

From Eqs. (4), it can seen that as ωt varies from $2\pi p$ to $2\pi(p + 1)$, where p is an integer, $F_0^{(1)}$ cy-

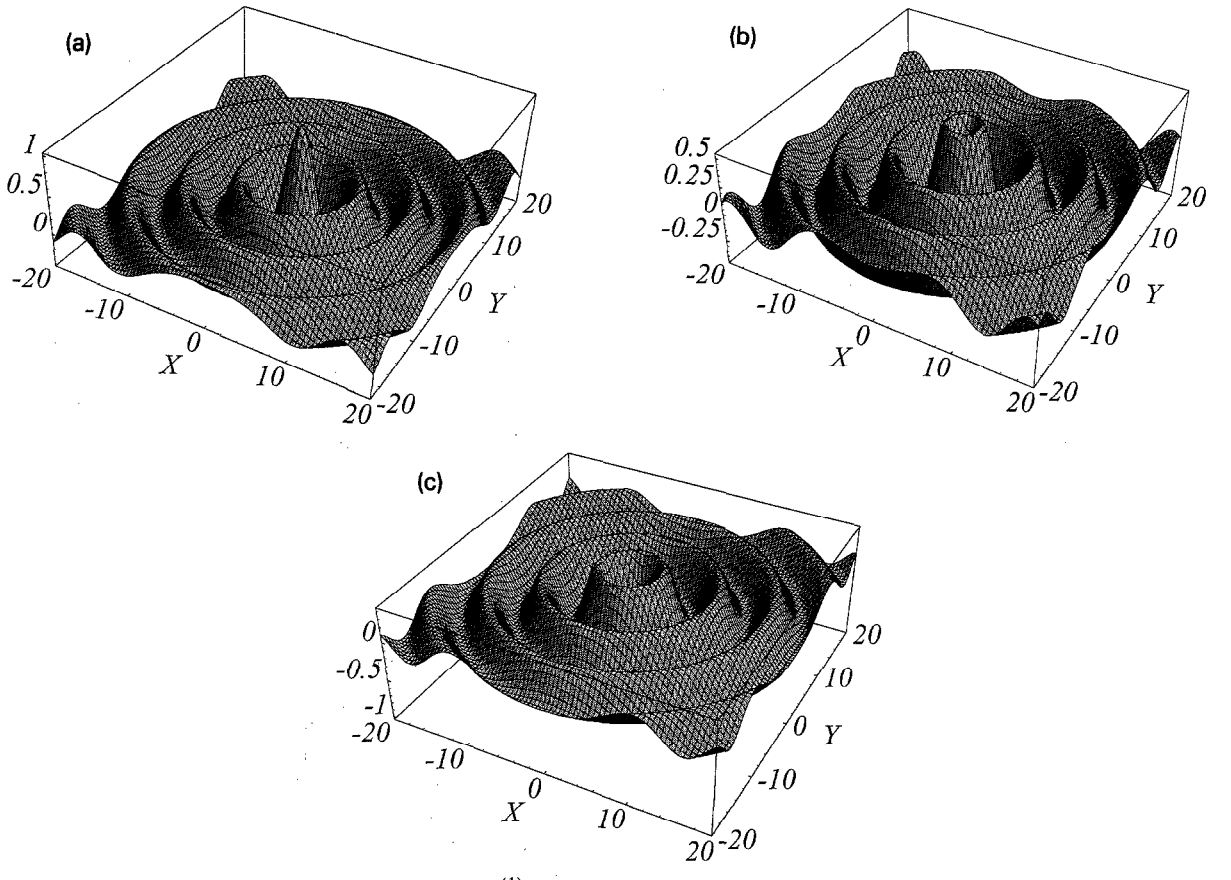

Fig. 1. Transverse profiles of the outgoing radial wave, $F_0^{(1)}$, of a zero order nondiffracting beam. The dimensionless transverse coordinates are (X,Y) such that $k_\rho \rho = \sqrt{X^2+Y^2}$. (a) $\omega t = 0$, $F_0^{(1)} = J_0(k_\rho \rho)$, (b) $\omega t = \pi/2$, $F_0^{(1)} = N_0(k_\rho \rho)$ and (c) $\omega t = \pi$, $F_0^{(1)} = -J_0(k_\rho \rho)$.

cles smoothly through the following series of patterns: $(J_0 \rightarrow N_0 \rightarrow -J_0 \rightarrow -N_0 \rightarrow J_0)$. During the same period $F_0^{(2)}$ cycles through the same patterns but in reverse order: $(J_0 \rightarrow -N_0 \rightarrow -J_0 \rightarrow N_0 \rightarrow J_0)$. A section of this temporal evolution is shown in Fig. 1, where $F_0^{(1)}$ is plotted for $\omega t = 0, \pi/2$ and π. From these snapshots of the transverse field, it can be deduced that $F_0^{(1)}$ is an outwardly travelling radially-symmetric wave. Since the profiles of $F_0^{(2)}$ are given by the same field patterns, but in reverse order, it follows that $F_0^{(2)}$ is the complementary wave travelling inwards. It should be quite evident that these travelling wave features arise directly from the inclusion of the Neumann functions.

The Neumann functions in Eqs. (3)–(4) are usually discarded because they possess a negative singularity at the origin; this feature would be apparent in Fig. 1b were it not concealed by the perspective of the diagram. However, singularities of this kind are common when radial symmetry is imposed on a solution; in this case, the feature can be interpreted physically as arising from the collapse of the incoming cylindrical wave on to the central axis which serves, simultaneously, as the source from which the outgoing wave emanates. To satisfy the boundary conditions at $\rho = 0$, each cylindrical wave must (in complex notation) be the complex conjugate of the other; this ensures that the imaginary (Neumann function) parts of the Hankel functions cancel out, leaving a Bessel function standing wave of finite amplitude. However, one would be wrong to infer from this that the Neumann functions are irrelevant, because their mediating role is immediately revealed whenever the steady state solution is disturbed, or (in a finite beam experiment) in

regions far from the axis where a steady state cannot in any case be established.

The first possibility is typified by the experiment described in [8] where the narrow central spot of a Bessel pattern was blocked by an obstacle on the $\rho = 0$ axis. A very short distance beyond the obstacle, the shadow region was observed to be filled in and the Bessel beam restored. When the transverse size of the central spot approaches λ, this process cannot be explained in terms of Fresnel diffraction theory. However, this effect can be explained in a natural way in terms of the ingoing Hankel wave.

To understand the second possibility, it is helpful to refer to Fig. 2 which shows the region in which nondiffraction effects can be observed in the experiment of Durnin et al. [1]. The source consists of a narrow annular ring of radius a followed by a collimating lens of focal length f. Each set of parallel rays drawn after the lens outlines the region where one of the Hankel waves exists, and the shaded cone indicates where the two waves overlap; it is only within this cone that the standing wave (Bessel function) profiles are formed and only here that the light remains nondiffracting. Beyond the cone, the field consists of the outgoing Hankel wave which continues to propagate away from the axis. For large values of $k_\rho\rho$, the wave is described by the asymptotic form of the Hankel function.

$$H_0^{(1)}(k_\rho\rho) \sim \frac{1}{\sqrt{k_\rho\rho}} \exp(\mathrm{i}k_\rho\rho). \tag{5}$$

The corresponding intensity diminishes as $1/k_\rho\rho$, whereas for an idealised Bessel beam the dependence goes as $\cos^2(k_\rho\rho)/k_\rho\rho$ [9]. Knowledge of the field pattern outside the cone of a zero order nondiffracting beam may not, initially, appear to be of particular significance. However, since in practice the cone must be of finite size, it is quite plausible that, in many of the proposed applications for nondiffracting beams, fixed arrays of nondiffracting probes, or two or more such beams with variable axis orientations, may be desirable. In these cases, an understanding of the interaction of adjacent beams, and the minimum separation required, necessitates such considerations.

The representation of zero order nondiffracting beams as travelling waves can be easily generalised to four dimensions by including the rapid longitudinal variation of the field, $\exp(-\mathrm{i}k_z z)$. In doing so, travelling cylindrical waves result in conical waves of total wavevector $\boldsymbol{k} = \boldsymbol{k}_\rho + \boldsymbol{k}_z$. It is this cone of wavevectors that appears in the integral formulation of Bessel beams [1,9]. With respect to the specific experimental configuration shown in Fig. 2, we have assumed that the illuminated circular slit is sufficiently narrow and that any diffractive edge waves from the aperture boundary are of negligible amplitude. In some experiments, these conditions may not be rigorously satisfied and additional oscillatory features in the transverse profile of the beam may result. However, this configuration is only one of many that can be used to generate nondiffracting beams and a full treatment which includes configuration-dependent higher order effects is outwith the scope of this paper. Instead, we have quantified the *generic* features of nondiffracting beams and our results may have application to *all* experimental configurations which have been used.

4. Rotating and spiral waves

We now turn our attention to higher order nondiffracting beams and, again, firstly consider the field patterns at longitudinal positions such that $\exp(-\mathrm{i}k_z z) = 1$. We repeat the procedure outlined in Section 3, now setting $E = H(\rho)\exp(\mathrm{i}m\phi)$. Incorporating the time dependence to find the total real field, yields the higher order Hankel waves as

$$\begin{aligned} F_m^{(1)} &= J_m(k_\rho\rho)\cos(\omega t - m\phi) \\ &\quad + N_m(k_\rho\rho)\sin(\omega t - m\phi), \\ F_m^{(2)} &= J_m(k_\rho\rho)\cos(\omega t - m\phi) \\ &\quad - N_m(k_\rho\rho)\sin(\omega t - m\phi). \end{aligned} \tag{6}$$

A correspondence with the zero order Hankel waves may be found by noting that when $\omega t - m\phi = (2 + p/2)\pi$ $(p = 0, 1, 2, 3, 4)$ the higher order waves cycle through a similar sequence of patterns: $(J_m \to N_m \to -J_m \to -N_m \to J_m)$ for $F_m^{(1)}$ and the reversed sequence for $F_m^{(2)}$. At any specific time, these patterns appear along lines of constant angle ϕ. Thus the higher order waves are not radially symmetric. Their functional dependence on $\omega t - m\phi$ shows them to be spatially inhomogeneous *rotating waves* (angular travelling waves). The temporal evolution of the transverse field patterns of $F_m^{(1)}$ and $F_m^{(2)}$ are illustrated in Fig.

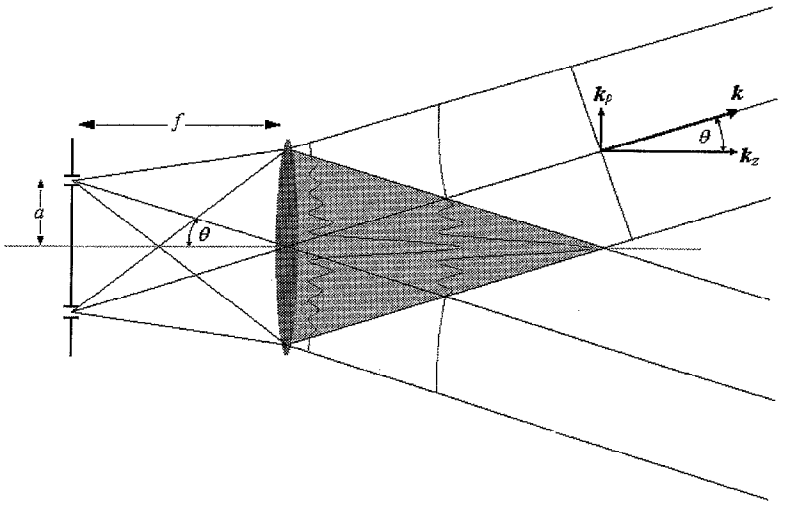

Fig. 2. Schematic of an experimental arrangement for creating nondiffracting beams. It is assumed that the collimating lens (having focal length f and radius $R > a$) is mounted in the aperture of an opaque sheet and that the illuminated circular slit (of width Δa and radius a) is sufficiently narrow: $\Delta a \ll \lambda f/R$. The evolution of a zero order Bessel function intensity profile in the conical region and the Hankel function profile outside this region is superimposed.

3. $F_5^{(1)}$ and $F_5^{(2)}$ are plotted for fixed z and $\omega t = 0$ and π. Parts (a) and (b) reveal the spiral nature of the higher order wave $F_m^{(1)}$. This wave has ridges of maximum amplitude which sweep out from the origin in an anti-clockwise direction. Considering the bright pattern at the centre of the beam, it can be clearly seen that the whole spiral pattern rotates in time. Parts (c) and (d) of Fig. 3 show that the second higher order Hankel wave is a counter-rotating spiral wave. In this case, ridges of high amplitude extend out into the plane in a clockwise direction.

As in the case of the zero order Hankel waves, one may generalise these concepts to include the longitudinal dimension. In this case, the higher order Hankel waves become

$$F_m^{(1)} = J_m(k_\rho\rho)\cos(k_z z + \omega t - m\phi) + N_m(k_\rho\rho)\sin(k_z z + \omega t - m\phi),$$
$$F_m^{(2)} = J_m(k_\rho\rho)\cos(k_z z + \omega t - m\phi) - N_m(k_\rho\rho)\sin(k_z z + \omega t - m\phi). \quad (7)$$

Since z can be seen to play an analogous role to t, one may consider the field to be a spiral wave which is rotating in time at fixed z, or vice-versa. Thus, a more accurate description of the field is that of a four-dimensional spiral wave.

The category of nondiffracting beams that we have considered so far has been restricted to the case where the electric field can be factorised as $E = H(\rho)\exp(-ik_z z + im\phi)$, where $H(\rho) = H_m^{(1)} + H_m^{(2)}$. Thus, $|E|^2 = |H(\rho)|^2$ and the intensity profile of such beams remains invariant during propagation. For both zero and higher order beams we find that the resultant profile is a radial standing wave. Interestingly, it is known that the superposition of two radial standing waves can result in a spiral wave [10]. Thus, it should be possible to construct another type of nondiffracting beam (for which the transverse intensity profile varies periodically in z) by superposition of a two or more distinct beams of the above type. Here, we consider the combination of two nondiffracting beams of the same carrier frequency, ω, whose individual axes of symmetry coincide. We do, however, allow the cones generated by each of the beams and the order of the Hankel waves to be distinct. Denoting the orders of the invariant nondiffracting beams as m and $m + n$ and their radial frequencies as k_ρ and k'_ρ, superposition results in a total electric field given by

$$E_T = \{H_m(k_\rho\rho) + H_{m+n}(k'_\rho\rho)\exp[\mathrm{i}(n\phi - \delta z)]\} \times \exp[\mathrm{i}(m\phi - k_z z)], \quad (8)$$

where

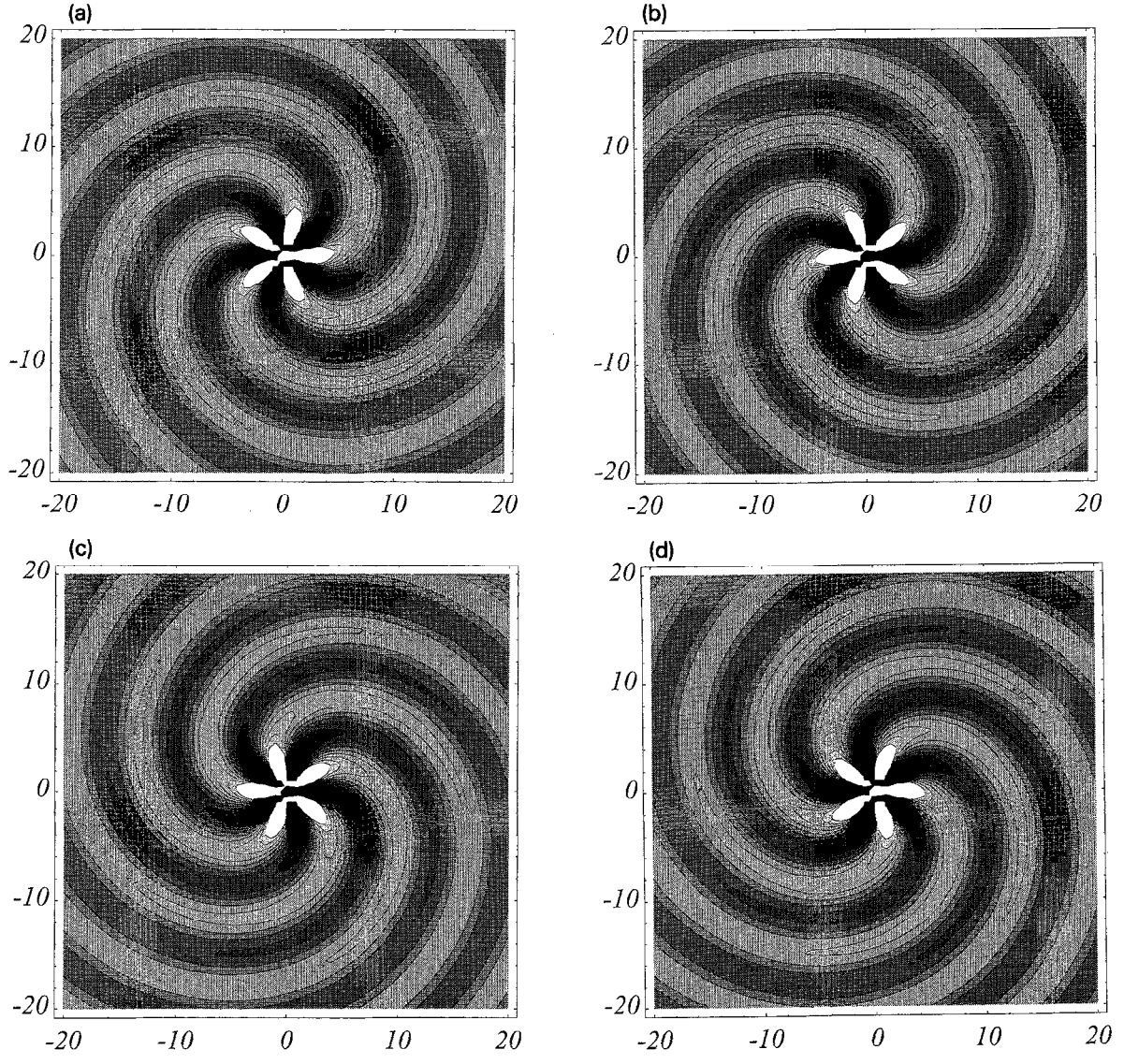

Fig. 3. Contours of the transverse profiles of the counter-rotating waves, $F_m^{(1)}$ and $F_m^{(2)}$, of a higher order nondiffracting beam. The dimensionless transverse coordinates are (X, Y) such that $k_\rho \rho = \sqrt{X^2 + Y^2}$ and $m = 5$ is plotted. At exactly $\rho = 0$ the field values are truncated to facilitate visualisation. Parts (a) and (b) show $F_5^{(1)}$ for $\omega t = 0$ and $\omega t = \pi$, respectively. In (c) and (d) the corresponding profiles of $F_5^{(2)}$ are given for $\omega t = 0$ and $\omega t = \pi$.

$$H_m(k_\rho \rho) = H_m^{(1)}(k_\rho \rho) + H_m^{(2)}(k_\rho \rho),$$

$$k_\rho^2 = k^2 - k_z^2 \quad \text{and} \quad k_\rho'^2 = k^2 - (k_z + \delta)^2.$$

For each separate beam, one may define a "collapse point" which occurs at the tip of the corresponding cone. We restrict our attention here to the field profiles which occur before the first collapse point on the z-axis. For convenience, we define a total normalised intensity which is given by $I_T = |E_T|^2/4$ and thus, for the superposition of the above two beams, one finds

$$I_T = \tfrac{1}{4} |H_m(k_\rho \rho) + H_{m+n}(k_\rho' \rho) \exp[\mathrm{i}(n\phi - \delta z)]|^2. \tag{9}$$

Boundary conditions dictate the regions where some, or all, of the Hankel waves are non-zero in the above expression. In the region where the two cones overlap all the constituent Hankel waves coexist ($H_m^{(1,2)}$ and $H_{m+n}^{(1,2)}$) and the intensity pattern can be written as

$$I_T = J_m^2(k_\rho\rho) + J_{m+n}^2(k'_\rho\rho) + 2J_m(k_\rho\rho)J_{m+n}(k'_\rho\rho)\cos(\delta z - n\phi). \quad (10)$$

Thus, for $n = 0$ (two constituent beams of the same Hankel order) superposition results only in a radial standing wave whose amplitude is modulated along the $z-$axis. However, for $n \neq 0$, the resulting beam is a rotating wave which possesses *finite angular momentum*. Fig. 4 illustrates the type of beams which may be generated. Here, we have set $m = 0, n = 3$ and $k'_\rho = 1.5k_\rho$. From the latter condition, it can be seen that the region where all the Hankel waves overlap is defined by the cone of the zero order beam (H_0). In parts (a) and (b) of this figure snapshots of the longitudinal evolution of the intensity profile in the overlap region are shown. Three bright lobes surround the central spot and the whole pattern rotates around the beam axis. Immediately outside of this overlap region the inwardly travelling components of the zero order cone are absent and thus the resulting transverse intensity pattern is different. One finds, for this region, that

$$I_T = \tfrac{1}{4}[J_m^2(k_\rho\rho) + N_m^2(k_\rho\rho)] + J_{m+n}(k'_\rho\rho)[J_m(k_\rho\rho)\cos(\delta z - n\phi) - N_m(k_\rho\rho)\sin(\delta z - n\phi)]. \quad (11)$$

Comparing this expression with Eqs. (6), one can deduce that, at fixed z, I_T is composed of a stationary radially symmetric pattern which has a rotating spiral wave pattern superimposed. In parts (c) and (d) of Fig. 4 the longitudinal evolution of I_T, as given by Eq. (11), is plotted. Since the transverse extent of the overlap region diminishes, in the direction of increasing z, one can envisage the evolution of the net intensity pattern in terms of two adjacent zones of the transverse plane; a shrinking central overlap region and a surrounding annular zone. More specifically, this can be accomplished by constructing a pattern composed of a central (circular) region, say from part (a) of Fig. 4, and the corresponding outer (annular) region at the same longitudinal position and time (part (c) of Fig. 4).

In the above considerations, angular motion develops along the longitudinal coordinate. However, precisely the same pattern evolution can also be generated in the time domain. If one relaxes the condition that the two constituent beams need to have the same carrier frequency, and denote the frequencies of the two beams as ω and $\omega+\Delta$, then Eqs. (9)–(11) generalise to include temporal evolution through the substitution $n\phi - \delta z \rightarrow n\phi - \delta z - \Delta t$. Thus, one can generate a four-dimensional rotating wave. Alternatively, one may choose between rotation in the temporal or spatial domain by either matching the cones or the carrier frequencies of the constituent beams.

5. Conclusions

A reformulation of nondiffracting beams, based on travelling wave solutions of the nonparaxial wave equation, has been presented. It is found that Bessel beams are a particular case of standing waves in a cylindrically symmetric coordinate system. We have proposed that the integral representation of nondiffracting beams is incomplete and we believe that we have presented compelling reasons for the introduction of Neumann functions into the solution. They enable a consistent description of the travelling wave features. Their incorporation has implications both in terms of the nature of nondiffracting beams and in terms of applications (the interaction with other beams or optical elements, for example). The on-axis singularity of the Neumann functions (when present in isolation) has been given a physical interpretation and it is shown that this singularity is cancelled out when counterpropagating Hankel waves coexist. This cancellation allows the electric field and the intensity to be finite at every point of the transverse plane. The more general formulation leads to expressions for the complete transverse profile of the electric field (generic descriptions of experimental realisations of nondiffracting beams). Outside the cone of the zero order nondiffracting beam, we find that there is a non-oscillatory decay of the field profile which is described by the first order Hankel function of zero order. For higher order beams the field profile decays according to the corresponding higher order Hankel function.

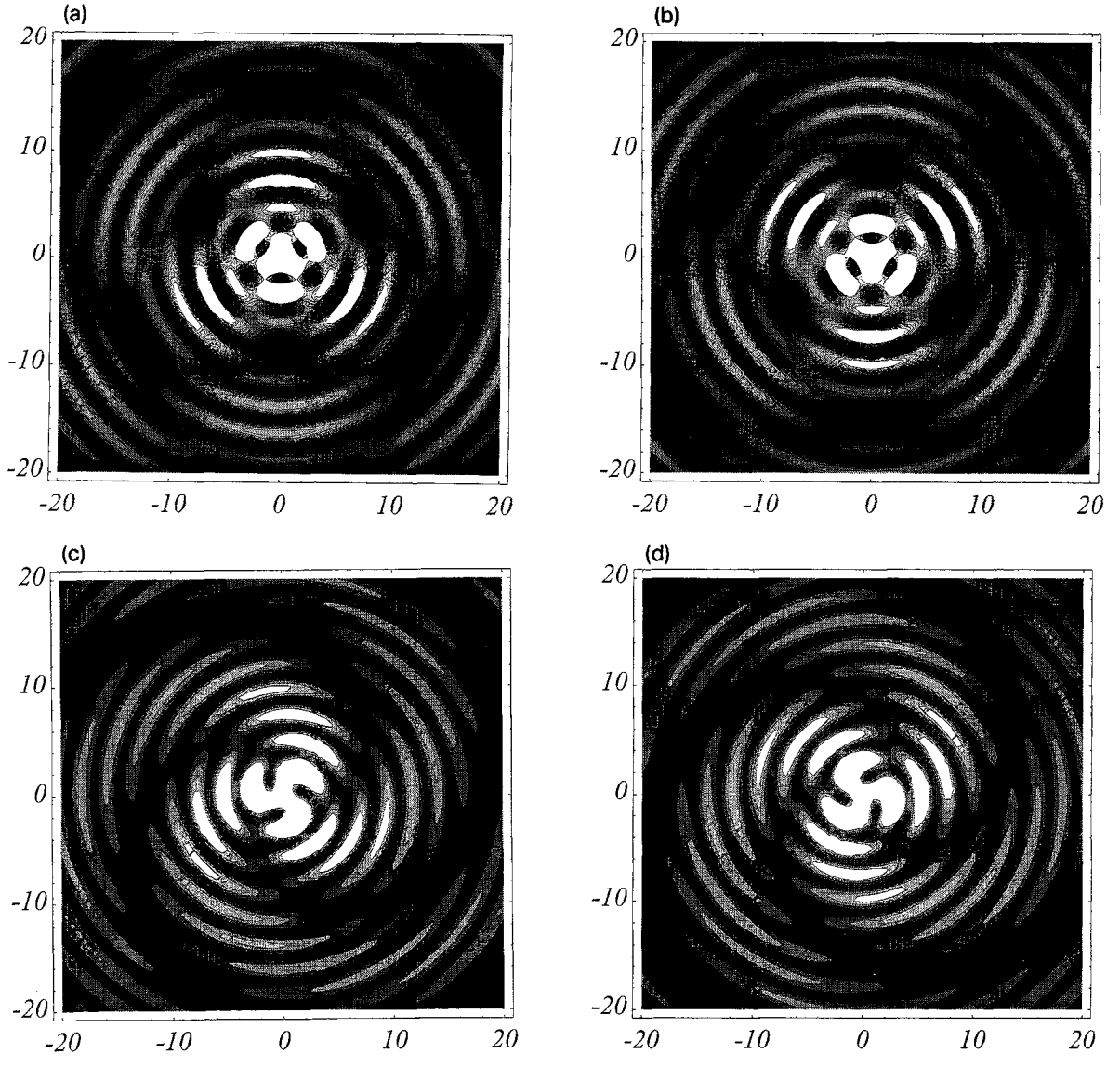

Fig. 4. Contours plots of transverse intensity profile. The parameters are $m = 0, n = 3$ and $k'_\rho = 1.5k_\rho$. The transverse scale is the same as that used in Figs. 1 and 3. Snapshots of the longitudinal evolution at fixed time are shown. (a) and (b) show profiles in the (periodically) nondiffracting cone of light for $\delta z = 0$ and $\delta z = \pi$, respectively. The function which defines the intensity patterns which appear immediately outside the inner light cone is plotted for the whole transverse plane in parts (c) and (d).

We have demonstrated that the superposition of two distinct nondiffracting beams can result in a periodically reconstructing beam with rotating and spiral wave features. This new class of beam could be termed "periodically nondiffracting". In fact, when only one carrier frequency is available, there exists an infinity of possible superpositions, involving zero order and higher order Hankel waves and a continuum of possible cone angles for each constituent beam. We have also shown that the rotating longitudinal evolution of such beams may be reproduced in the time domain by using constituent beams which have the

same cone angle but distinct carrier frequencies. Periodically nondiffracting beams which possess rotating wave characteristics may find use in applications which, for example, utilise a finite angular momentum of the light beam to manipulate small particles. Of course, the complexity of the transverse intensity profiles of such beams, and their speed of rotation, can be prescribed for any particular application. In this paper we have restricted our attention to nondiffracting beams which are defined by, or derived from, the ansatz $E = H(\rho)exp(-ik_z z + im\phi)$. Our findings are suggestive of the existence of a much wider class of periodically nondiffracting beams. Further investigations are merited in which the rigid contraints of the above ansatz are systematically relaxed.

In previous studies of the propagation of phase singularities and optical vortices [11] it was found that Gaussian beams which have a phase singularity evolve, during linear propagation, in such a way that the spiral wave structure of the field essentially diffracts out and is destroyed. It was found necessary to launch such a beam into a (self-defocusing) nonlinear medium to preserve the spiral field pattern. However, we have shown here that, for beam profiles which are periodically nondiffracting, spiral and rotating wave patterns which possess phase singularities may propagate stably in linear media.

Acknowledgements

The authors would like to thank Dr Jorge Ojeda-Castaneda for useful discussions. This work was supported in part by UK SERC grant no. GR/J04746, UK EPSRC grant no. GR/K54748 and funds from CONACYT (Mexico), INAOE (Mexico) and CVCP-ORS (UK).

References

[1] J. Durnin, J.J. Miceli Jr. and J.H. Eberly, Phys. Rev. Lett. 58 (1987) 1499;
J. Durnin, J. Opt. Soc. Am. A 4 (1987) 651.
[2] Y. Lin, W. Seka, J.H. Eberly, H. Huang and D.L. Brown, Appl. Optics 31 (1992) 2708.
[3] N. Davidson, A.A. Friesen and E. Hasman, Optics Comm. 88 (1992) 326;
A.J. Cox and J. D'Hanna, Optics Lett. 17 (1992) 232.
[4] T. Wulle and S. Herminghaus, Phys. Rev. Lett. 70 (1993) 1401.
[5] S. Chávez-Cerda, Self-confined Beam Propagation and Pattern Formation in Nonlinear Optics, Ph.D. Thesis, Imperial College of Science, Technology and Medicine, University of London (1994).
[6] M. Born and E. Wolf, Principles of Optics, 6th Edition (Pergamon Press, Oxford, 1980).
[7] George Arfken, Mathematical Methods for Physicists, 3rd Edition (Academic Press, San Diego, 1985).
[8] R.M. Herman and T.A. Wiggins, J. Opt. Soc. Am. A 8 (1991) 932.
[9] P.W. Milonni and J.H. Eberly, Lasers (Wiley, New York, 1988).
[10] P.H. Ceperley, Am. J. Phys. 60 (1992) 938.
[11] G.S. McDonald, K.S. Syed and W.J. Firth, Optics Comm. 94 (1992) 469.